Research Article | Vol. 10, No. 1 | 1 Jan 2019 | BIOMEDICAL OPTICS EXPRESS 215
Biomedical Optics EXPRESS

Side-polished flexible SPR sensor modified by graphene with *in situ* temperature self-compensation

PENGHAO ZHANG,[1] BINGYU LU,[1] YANWEN SUN,[2] HAIXIA YU,[2,3] KEXIN XU,[1] AND DACHAO LI[1,4]

[1]*State Key Laboratory of Precision Measuring Technology and Instruments, Tianjin University, 300072, China*
[2]*Tianjin Key Laboratory of Biomedical Detecting Techniques and Instruments, Tianjin University, 300072, China*
[3]*hxy2081@tju.edu.cn*
[4]*dchli@tju.edu.cn*

Abstract: Fiber-based techniques make it possible to implant a miniaturized and flexible surface plasmon resonance (SPR) sensor into the human body. However, for implantable applications, the miniaturization of fiber SPR sensors results in low sensitivity compared with traditional prism-type SPR sensors due to limited space and the effects of temperature fluctuations. Therefore, it is necessary to compensate for temperature drift in the measurements, such as the case of the quantification of the relationship between glucose concentration and SPR resonance wavelength. In this report, we proposed a highly sensitive fiber SPR sensor based on a side-polished structure modified by graphene for implantable continuous glucose monitoring with *in situ* temperature self-compensation using a long-period fiber grating (LPFG). The results demonstrate that the sensor with monolayer graphene achieved the best sensitivity of 3058.22 nm/RIU, and the LPFG achieves a maximum resolution of 0.042 nm/°C. The proposed SPR sensor enabled the detection of hypoglycemia, which is still a significant challenge for continuous glucose monitoring in a clinical setting.

1. Introduction

Diabetes mellitus is a common chronic disease that requires continuous monitoring of blood glucose level to provide guidance for diagnosis and therapy [1,2]. Nowadays, implantable enzyme electrode sensors are widely used for continuous glucose monitoring in a clinical setting, but this approach has inherent disadvantages which include significant current signal drift due to the bioelectricity of the body. The method may also fail to detect hypoglycemia as a result of the irreversible consumption of glucose during the process of enzyme catalytic reaction [3]. The implantable fiber SPR sensor is able to overcome these drawbacks due to the following characteristics [4]. First, the fiber SPR sensor is the only part that is implanted in the subcutaneous tissue, and only the optical signal passes through the tissue. Therefore, the glucose measurement is not affected by the bioelectricity of the body. Thus, the resulting reduced signal drift would facilitate more accurate glucose measurement results [5]. Second, glucose determination based on refractive index variation guarantees that no glucose is depleted during the measurement process which is critical in the detection of hypoglycemia, which is still a significant challenge with regard to continuous glucose monitoring using an enzyme electrode sensor [6]. Third, the implantable fiber SPR sensor could allow for a flexible connection to the subcutaneous tissue, thereby facilitating the acquisition of a more stable and accurate signal [7].

However, the miniaturization of fiber SPR sensor results in a low sensitivity compared with traditional prism-type SPR sensors. To address this problem, current research activity is mainly focused on effective methods to fabricate nanostructures such as noble metal

#340352 https://doi.org/10.1364/BOE.10.000215
Journal © 2019 Received 25 Jul 2018; revised 23 Nov 2018; accepted 4 Dec 2018; published 17 Dec 2018

Biomedical Optics EXPRESS

nanoparticles or two-dimensional materials on the surface of fiber SPR sensors, to stimulate localized surface plasmon resonance for enhancement of the sensitivity of the SPR sensor [8–10]. It is still a significant challenge to construct nanostructures on the micron-scale on the cylindrical surface of a fiber SPR sensor [11]. Therefore, the side-polished structure which is close to a prism structure, is preferred instead of a cylindrical fiber with respect to sensors sensitivity and modification difficulty.

In recent years, graphene has attracted great attention because of its distinctive electrical and optical properties [12,13]. It can significantly increase the mobility of electrons on the gold film of the SPR sensor, since the charge carrier mobility of graphene is reported to be as high as 10^6 cm^2 V^{-1} s^{-1} and it is known as the best conductor to date [12,14]. In addition, it can serve as biomolecular recognition elements to enhance the adsorption of biomolecules on the gold film of SPR sensors because of its large surface area and pi-stacking force [15–17], which could overcome the sensitivity limit of the SPR biosensor due to the poor adsorption of gold to biomolecules. In addition, chemical vapor deposition (CVD) graphene has more advantages compared to graphene prepared by oxidation-reduction methods including a better structure. Moreover, the size of graphene is not limited by ingredients, which has further promoted the adoption of graphene-based biosensors. Thus, the utilization of graphene which can enhance the electron mobility of gold and adsorption of glucose molecules to achieve high sensitivity of refractive index-based detection [18], will improve the accuracy of glucose measurement in trace glucose solution. Zhang presented a U-bent fiber optic SPR sensor based on graphene/AgNPs, which combined the advantages of graphene, AgNPs, and a U-bent fiber to achieve a sensitivity of 1198 nm/RIU [19]. Yang proposed a photonic crystal fiber (PCF)-based SPR sensor with a wavelength sensitivity of 2520 nm/RIU [20]. Based on the remarkable properties of graphene, we designed a high sensitivity fiber SPR sensor with a side-polished structure for easy modification of CVD graphene, which can promote the electron mobility of gold and the adsorption of a glucose molecule to achieve high sensitivity of refractive index-based detection [18].

The resonance wavelength of SPR is also susceptible to the analyte temperature. As Yang et al. reported, the resonance wavelength of traditional SPR temperature sensors exhibits a blue shift as the temperature increases [21]. Therefore, fluctuations of the body temperature could affect the measurement accuracy of glucose concentration after the sensor is implanted into the subcutaneous tissue [22]. For traditional prism-based SPR sensors, a temperature control device such as a thermal box or platinum electrode is typically used to measure and maintain a stable temperature during experiments [23]. However, it is impossible to implant a temperature control device into the body because of volume and biocompatibility constraints. Therefore, there is great significance in *in situ* measurements accompanied by temperature compensation. Since the first long-period grating (LPFG) was successfully inscribed on an optical fiber in 1996 [24], it has been widely used for temperature measurement. LPFG temperature sensors can be used in environments with high electromagnetic interference such as in the presence of bioelectricity, and in instances where space is strictly limited because of constraints such as small size, lightweight, and flexible; as well as high radiation tolerance. For the current SPR sensor, we cannot determine whether the change of the resonance wavelength is caused by temperature or is solely due to concentration changes, in the case of the SPR sensor. Therefore, we engraved the LPFG onto the fiber core to incorporate a temperature sensor inside the SPR sensor such that *in situ* temperature and concentration can be obtained simultaneously to compensate for the temperature drift of the SPR spectrogram.

2. Fabrication of the SPR sensor with temperature self-compensation

The proposed fiber SPR sensor that is engraved onto the fiber core with a LPFG modified with graphene for continuous glucose monitoring is shown in Fig. 1(A). A cellulose acetate semi-permeable membrane with a selectable molecular weight cut-off was used as a protective cover to separate the implanted sensor from the tissue and further filter out large

Biomedical Optics EXPRESS

biological molecules within the interstitial fluid (ISF), thereby allowing glucose molecules to pass through [25]. Single mode fiber with coating diameter of 242um, cladding diameter of 125um and core diameter of 8.2um (Corning SMF28) was used in this paper. The distance of the long-period fiber grating (LPFG) from the side polished portion of the fiber is about 30mm. The residual thickness of the cladding is 0 um, the length of the polished region is 5 mm, the thickness of the gold film is 35 nm, and the thickness of the chromium layer is 4 nm. These optimal parameters were chosen via simulation [26].

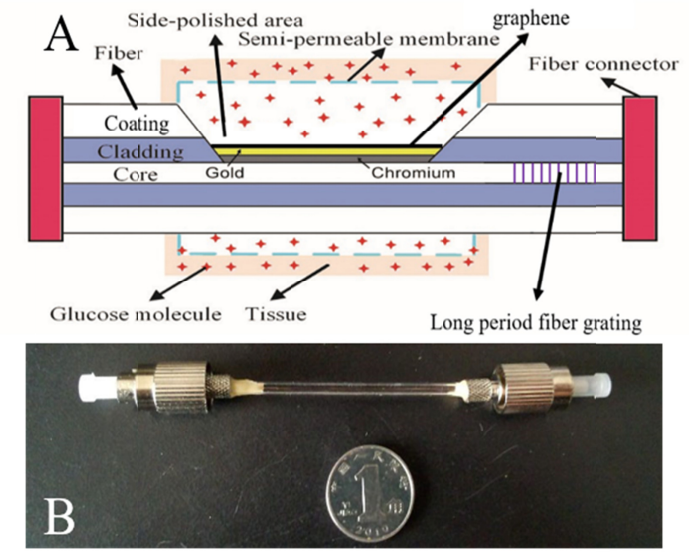

Fig. 1. Schematic of the side-polished SPR sensor with LPFG (A), Photo of the side-polished SPR sensor after packaging (B).

The fiber sensor was fabricated in four steps. Firstly, the fiber grating was engraved utilizing a CO_2 laser. Secondly, the cladding layer of one side of the cylindrical fiber was polished off for easy surface modification. Then, gold and chromium films were deposited on the side-polished area via physical vapor deposition. Finally, different layers of CVD graphene were transferred onto the gold film by a liquid transfer method to promote the electron mobility of gold and adsorption of a glucose molecule to promote high sensitivity of refractive index-based detection. Figure 1(B) shows the photo of the side-polished SPR sensor after packaging. The length of the fiber sensor is about 10cm, the optical fiber connector is SMA905, and the sensing area was fixed with half-glass tube.

2.1 Engraving the LPFG using a CO_2 laser

The LPFG was engraved into the fiber core utilizing a point by point writing technique with a CO_2 laser, which can easily control the period of the LPFG. (The LPFG in this investigation was fabricated by Guangzhou iridium Photoelectric Technology Co., Ltd.) This method can cause densification, and residual stress could introduce larger refractive index change to the fiber core. The resonance wavelength of the LPFG is determined by the grating period and pitch, and is susceptible to the surrounding temperature. (LPFG length: 20 mm, period: 553 μm).

2.2 Polishing the fiber SPR sensor on one side

The process of specific operation are as follows: Firstly, the fiber is fixed and attached to the side of the grinding wheel. Then, the optical fiber is straightened. When the grinding wheel

Biomedical Optics EXPRESS

turns, the cladding on the side of the fiber is eroded. Meanwhile, the specific grinding thickness is calibrated using a microscope and the relationship between the calibrated thickness and the insertion loss of the optical fiber is established. In the process of polishing, the insertion loss of the optical fiber will is detected in real time. When the predetermined insertion loss is achieved, the process is immediately terminated. A series of mechanical operations, such as the start and stop of the rotation of the grinding wheel are controlled by a computer. Thus enhances the precision and accuracy of the processing process. After polishing the fiber, the polishing area should be further polished to make the surface smooth to ensure the thickness of the metal layer is uniform in the next step which can enhance the phenomenon of SPR. One side of the fiber presents a relatively flat slope in the transition region, rather than a strict plane. The length of the side-polished area is 5 mm and the residual thickness of the cladding in the area is 0 μm, which means that part of the core is exposed to the air.

2.3 Physical vapor deposition of chromium/gold

The SPR phenomenon requires a metal film to generate surface plasma waves. In this report, chromium (as a transition layer to increase the fastness of the gold film and quartz) and gold were used to stimulate the SPR effect. The preparation materials for vacuum coating are: chromium wire, gold wire with a purity of 99.999%, a molybdenum boat, as well as a fixture for coating. Moreover, this investigation used the LN-284SA vacuum coating machine produced by Shenyang Lining company to meet the requirements for the thicknesses of the chromium layer and the gold film of 4 nm and 35 nm, respectively.

2.4 Graphene modification by liquid transfer method

It is very difficult to grow graphene directly on the micro-scale sensing area of fiber SPR sensor after polishing. So a liquid transfer method was proposed to grow CVD graphene onto the Au film.

Single-Layer graphene (ACS MATERIAL, USA) was transferred onto the side-polished surface in deionized water according to the steps outlined in Fig. 2(A). Firstly, the graphene on polymer was released into the deionized water which leads to the separation of the polymer and single-layered graphene. Secondly, the graphene was salvaged by depositing it on filter paper. Then the paper with the deposited single-layer graphene was cut into pieces with the desired shape and size. Subsequently, the desired pieces were returned to the deionized water and subsequently captured with the cleaned fiber SPR sensor to allow the graphene to cover the side-polished surface exactly. Finally, the PMMA (polymethyl methacrylate) layer was cleared by acetone [27].

The details of process (f) in Fig. 2(A) is shown in Fig. 2(B). The graphene film floats on the surface of the water just above the fiber before the transfer process, as shown in Fig. 2(B). Then, the graphene descends with the decline of the surface of the water and gradually adheres to the side-polished surface until the water is completely removed using a Pasteur pipette due to Van der Waals forces. Finally, the PMMA layer is removed with acetone and a new CVD single-layer graphene can be transferred to the previous graphene layer through the same method. Once the graphene has been wrapped around the fiber, it does not separate from its surface even after immersion in water because of the high bond energy of graphene. This method could be used in the transfer of multi-layer graphene as well. Figure 2(C) shows the characterization of graphene on the surface of the SPR sensor using Laser Micro-Raman Spectrometry with a 532 nm light source. Figure 3 shows the SEM images of the proposed sensor with different layers of graphene. From Fig. 3(B) to Fig. 3(D), we can see the boundary of transferred CVD graphene, and the color gradually deepened as the layers increased. The results prove that the proposed transfer method is reliable and effective.

Biomedical Optics EXPRESS

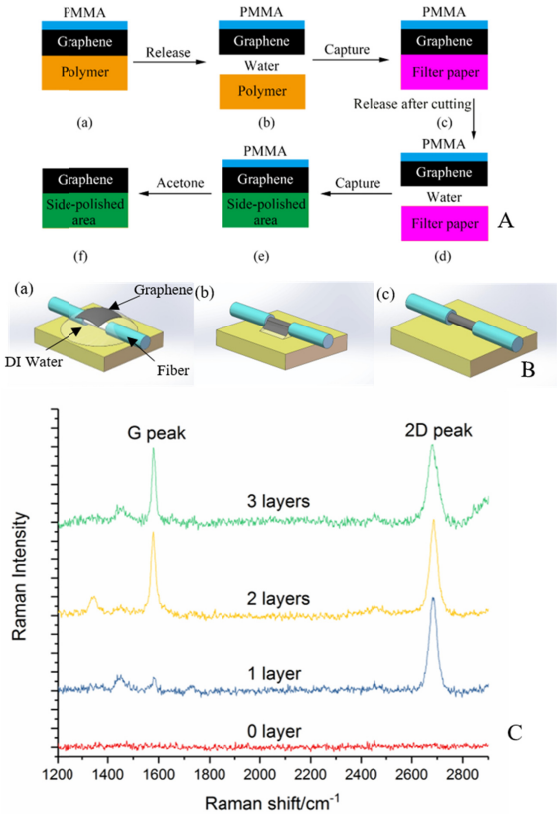

Fig. 2. Transferring process of graphene (A), the decoration of CVD single-layer graphene film by liquid transfer method (B) and the characterization of graphene on the surface of SPR sensor (C).

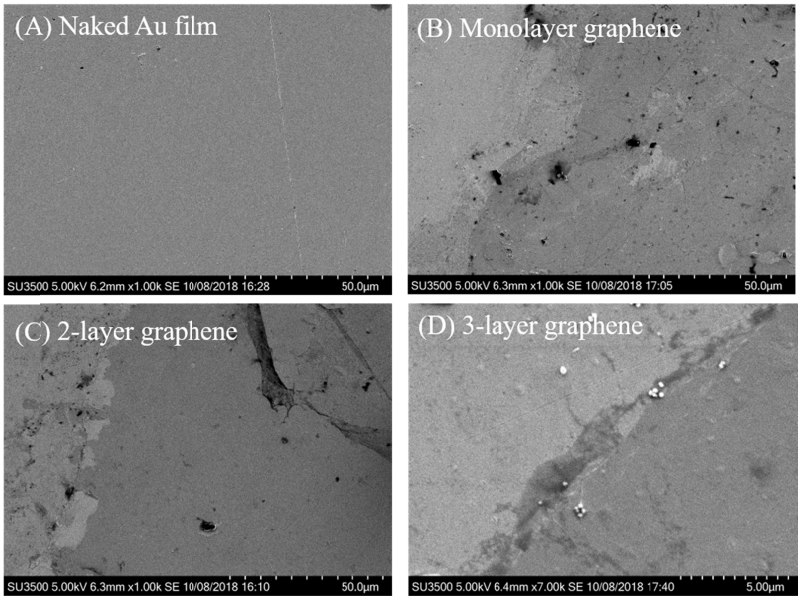

Fig. 3. SEM images of the fabricated sensor layer by layer.

Biomedical Optics EXPRESS

3. Results and discussion

3.1 Experimental system

A schematic of the experimental system is shown in Fig. 4(A). The light from a supercontinuum white laser source is coupled into the core of the proposed fiber SPR sensor. Then the spectra of the sensor were measured using a commercial spectrometer USB2000 (wavelength range: 300~1100nm). In the experiment, the sensor was placed in a deionized water bath with a temperature controller. To obtain the precise temperature information at the sensor's location in real time, a Pt electrode (PT100) capable of high-accuracy temperature measurements was placed in close proximity to the side-polished area of the sensor, in the water. Before the experiment, the relationship between the temperature of the glucose solution and resistance was determined for calibration purposes. When the temperature of the glucose solution was 35°C and 42°C, the corresponding resistance was 117.70 Ω and 120.73 Ω. In the temperature range from 35°C to 42°C, the nonlinear error of PT100 is negligible. In our study, the experiment was performed in a temperature range of 35-42°C (Δ = 0.5°C, to cover the normal body temperature range). For the majority of healthy individuals, normal blood sugar levels are as follows: Between 3.9 to 6.1 mmol/L (70 to 110 mg/dL) when fasting. Up to 7.8 mmol/L (140 mg/dL) 2 hours after eating. Thus, the experimental concentration range of glucose was 0-300mg/dL.

3.2 Temperature measurement by LPFG

The relationship between temperature and resonance wavelength is shown in Fig. 4(B) (the R-square of the fitting curve was 0.99314). When the temperature was increased from 35°C to 42°C, the resonance wavelength shifted from 1546.63 nm to 1546.924 nm. Because of the perfect linearity of the relationship curve, the temperature information can be easily obtained by measuring the resonance wavelength of the LPFG.

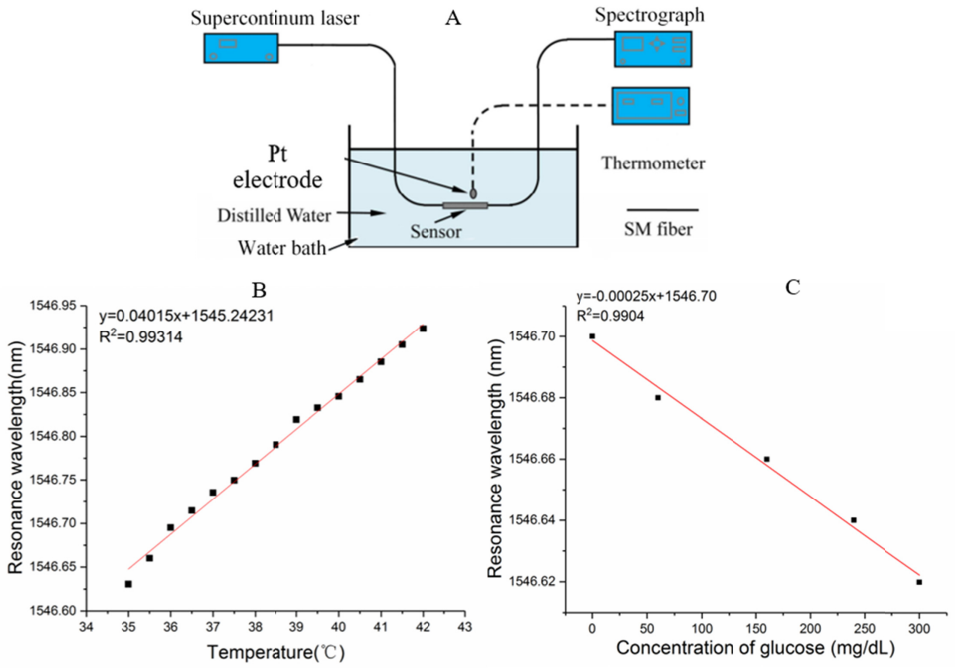

Fig. 4. The schematic of experimental system (A), the resonance wavelength of LPFG versus temperature (B) and the resonance wavelength of LPFG versus concentration of glucose at 36°C (C).

Biomedical Optics EXPRESS

3.3 Temperature versus resonance wavelength of SPR

The relationship between temperature and resonance wavelength of the deionized water measured by the SPR sensor modified with 0, 1, 2, and 3 layers of graphene is shown in Fig. 5. Before measurement, the solution was heated to a higher temperature, then the temperature of the solution drops naturally. When the temperature decreased from 42°C to 35°C, it introduced a red shift in the resonance wavelength of the SPR sensor. Figure 5(B) shows the sensor modified with a monolayer of graphene has a smaller error bar and better linearity compared with the other groups. This implies that the data is more stable and the variation of resonance wavelength with the change of temperature is more uniform. This is an important point in the process of temperature compensation.

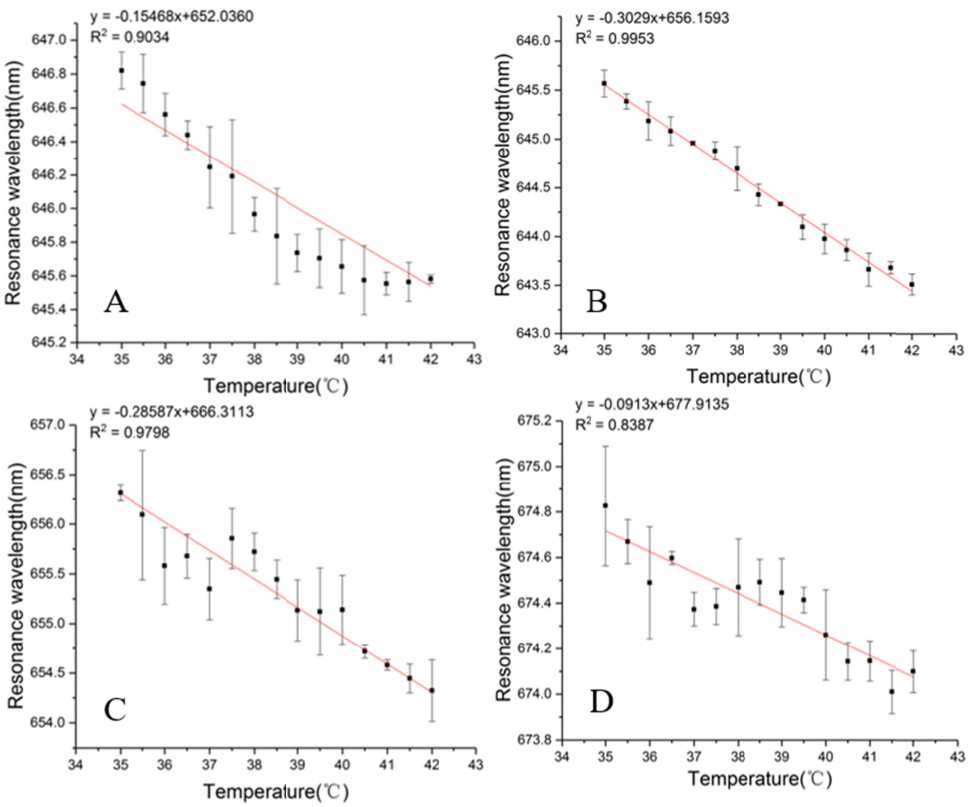

Fig. 5. The resonance wavelength of deionized water measured by SPR sensor modified with 0-layer graphene (A), monolayer (B), two-layers (C) and three-layers graphene (D) versus temperature.

3.4 Number of CVD graphene layer versus resonance wavelength of SPR

The relationship between the resonance wavelengths associated with glucose concentration measured by the SPR sensor is shown in Fig. 6(A). Table 1. shows the effects of the different number of graphene layer with respect to sensitivity, and a comparison with the proposed sensor and previously reported fiber SPR sensors. These sensor measurements at 36°C are modified with 0, 1, 2, and 3 layers of graphene. It is reported that the sensitivity of SPR sensors increases with the number of graphene layers due to adsorption of biomolecules of carbon based-ring structures. However, the increase in the thickness of graphene also introduces damping of the surface plasmon oscillations due to graphene's finite imaginary component of the dielectric constant. It was determined that the sensor with monolayer

Biomedical Optics EXPRESS

graphene achieved the best sensitivity of 3058.22 nm/RIU during the experiments. This value represents an enhancement of 2.29 times compared with the sensitivity of 1333.63 nm/RIU for the control group without graphene. To ensure the reliability of experimental data, the measurement uncertainty of SPR sensor modified with monolayer graphene at different glucose concentration as shown in Table 2.

Table 1. The Sensitivity comparison with the proposed sensor and previously reported fiber SPR sensors

	Sensitivity (nm/RIU)	R-Square
w/o graphene	1333.63	0.9886
1-layer graphene	3058.22	0.9994
2-layers graphene	2358.28	0.9888
3-layers graphene	1572.86	0.9826
U-bent fiber optic SPR sensor with graphene/AgNPs [19]	1198	
PCF-based SPR sensor [20]	2520	

Table 2. The measurement uncertainty of SPR sensor modified with monolayer graphene

Concentration of glucose (mg/dL)	Average (nm)	Standard deviation (σ_x)	Uncertainty (%)
0	644.9867	0.195253	8.732263
10	644.7336	0.053005	2.370515
20	648.2094	0.216827	9.697103
40	648.5055	0.06615	2.958401
60	648.8958	0.064969	2.905589
80	651.1505	0.026071	1.165967
100	652.4212	0.030582	1.367727
150	655.8866	0.04319	1.931578
200	657.4944	0.172456	7.712713
250	657.3093	0.074062	3.31227
300	661.6141	0.031968	1.429709

3.5 The temperature compensation of SPR resonance wavelength

Figure 4(C) shows the relationship between LPFG resonance wavelength and glucose concentration at 36°C. When the glucose concentration increased from 60 to 160mg/dL (to cover the normal blood sugar range), the resonance wavelength shifted from 1546.68 nm to 1546.66 nm. Compared to the change of resonance wavelength caused by temperature, glucose concentration has smaller effect on resonance wavelength. Therefore, the LPFG was relatively insensitive to the ambient RI changes in our experiments but was sensitive to changes in the ambient temperature. The SPR exhibited sensitivity to both changes. The temperature spectrum and SPR spectrum are separated so that a spectrogram which covers both spectra can be obtained simultaneously as shown in Fig. 6(B) and Fig. 6(C). Thus, the temperature of the solution can be obtained by LPFG and the drift of the resonance wavelength caused by temperature can be compensated.

In the temperature compensation experiment, 36°C was set as the standard temperature. At first, the resonance wavelength of the LPFG was measured and the experimental temperature could be obtained as shown in Fig. 4(B). Then the resonance wavelength of the SPR (λ_1) at 36°C could be obtained by inserting 36°C into the fitting formula of Fig. 5(B). Finally, the pure resonance wavelength shift of the SPR caused only by the glucose concentration could be calculated by subtracting λ_1 from λ_i [28] (As the glucose concentration is increased in each subsequent measurement, the temperature of the system is also correspondingly raised by 0.5 degrees C) as shown in Fig. 6(D). Prior to temperature compensation, the blue-shift of the resonance wavelength increases as temperature rises, which results in the inaccuracy of the glucose concentration measurement. After temperature

Biomedical Optics EXPRESS

compensation, the drift of the resonance wavelength can be eliminated (the R-square of the fitting curve was 0.9987).

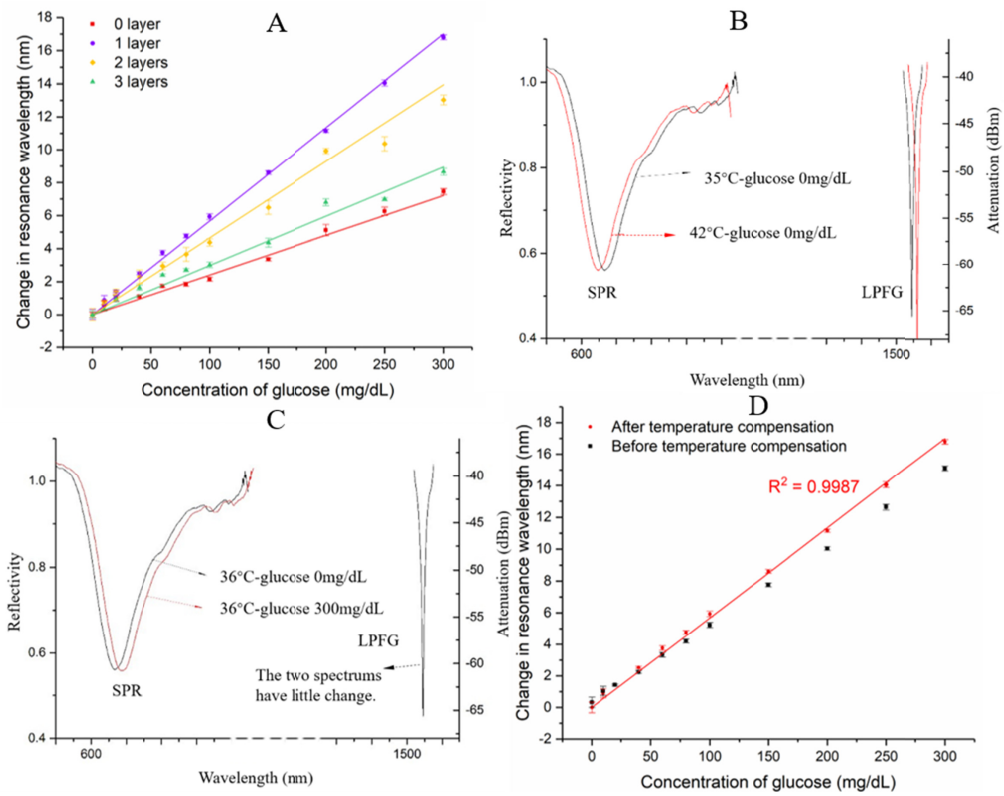

Fig. 6. The resonance wavelength of SPR modified with different number of CVD graphene layer versus concentration of glucose at 36°C (A), the spectrum of SPR and LPFG at different temperature and deionized water (B), the spectrum of SPR and LPFG at different glucose concentration and fixed temperature of 36°C (C), and the SPR resonance wavelength measured by experiments at different glucose concentration and different temperature, and the pure resonance wavelength shift caused only by glucose concentration after temperature compensation (D).

4. Conclusion

In this investigation, a side-polished fiber was designed to create a plane sensitive area for easier modification of graphene compared to a cylindrical fiber. The SPR sensor with monolayer graphene achieved the best sensitivity of 3058.22 nm/RIU, which has a nearly 2.29 times enhancement when compared to the SPR sensors without treatment. In addition, we were able to obtain exact temperatures using a LPFG engraved into the fiber core of the SPR sensor. During the temperature range from 35°C to 42°C, which cover the normal body temperature, the relationship between the resonance wavelength of the LPFG and the temperature was linear, and the LPFG could achieve a maximum resolution of 0.042 nm/°C. After temperature compensation, the pure resonance wavelength of the SPR caused only by changes in glucose concentrations, was obtained. The experiment results showed that this method could detect temperature accurately and compensate for the drift of SPR resonance wavelength caused by body temperature changes, considering that there are many components in the ISF which contribute to the value of the refractive index. A borate polymer which can modify the surface of the SPR sensor and specifically adsorb glucose molecules has been synthesized [26]. Tests on the surface modification of a fiber SPR sensor with borate polymer are on-going and will be published in the future.

Biomedical Optics EXPRESS

Funding

National Key R&D Program of China (2017YFA0205103); National Natural Science Foundation of China (No.81571766 and No.61428402); Natural Science Foundation of Tianjin (No. 17JCYBJC24400); the 111 Project of China (No. B07014).

Disclosures

The authors declare that there are no conflicts of interest related to this article.

References

1. C. Zecchin, A. Facchinetti, G. Sparacino, G. De Nicolao, and C. Cobelli, "A New Neural Network Approach for Short-Term Glucose Prediction Using Continuous Glucose Monitoring Time-Series and Meal Information," Conf. Proc. IEEE Eng Med Bio Soc. **2011**, 5653–5656 (2011).
2. Y. J. Lee, J. D. Kim, and J. Y. Park, "Flexible enzyme free glucose micro-sensor for continuous monitoring applications," in *Solid-State Sensors, Actuators and Microsystems Conference, 2009, TRANSDUCERS 2009. International* (2009), pp. 1806–1809.
3. G. Schmelzeisen-Redeker, A. Staib, M. Strasser, U. Müller, and M. Schoemaker, *Overview of a Novel Sensor for Continuous Glucose Monitoring* (SAGE, 2013).
4. D. Li, B. Lu, R. Zhu, H. Yu, and K. Xu, "An optofluidic system with volume measurement and surface plasmon resonance sensor for continuous glucose monitoring," Biomicrofluidics **10**(1), 011913 (2016).
5. P. Polynkin, A. Polynkin, N. Peyghambarian, and M. Mansuripur, "Evanescent field-based optical fiber sensing device for measuring the refractive index of liquids in microfluidic channels," Opt. Lett. **30**(11), 1273–1275 (2005).
6. J. D. Newman and A. P. Turner, "Home blood glucose biosensors: a commercial perspective," Biosens. Bioelectron. **20**(12), 2435–2453 (2005).
7. Z. Pu, R. Wang, J. Wu, H. Yu, K. Xu, and D. Li, "A flexible electrochemical glucose sensor with composite nanostructured surface of the working electrode," Sens. Actuators B Chem. **230**, 801–809 (2016).
8. D. Li, Y. Sun, S. Yu, C. Sun, H. Yu, and K. Xu, "A single-loop fiber attenuated total reflection sensor enhanced by silver nanoparticles for continuous glucose monitoring," Sens. Actuators B Chem. **220**, 1033–1042 (2015).
9. J. K. Nayak, P. K. Maharana, and R. Jha, "Dielectric over-layer assisted graphene, its oxide and MoS2-based fibre optic sensor with high field enhancement," J. Phys. D Appl. Phys. **50**(40), 405112 (2017).
10. A. K. Mishra, S. K. Mishra, and R. K. Verma, "Graphene and Beyond Graphene MoS2: A New Window in Surface-Plasmon-Resonance-Based Fiber Optic Sensing," J. Phys. Chem. C **120**(5), 2893–2900 (2016).
11. A. M. Shrivastav, S. K. Mishra, and B. D. Gupta, "Localized and propagating surface plasmon resonance based fiber optic sensor for the detection of tetracycline using molecular imprinting," Mater. Res. Express **2**(3), 035007 (2015).
12. A. H. Castro Neto, F. Guinea, N. M. R. Peres, K. S. Novoselov, and A. K. Geim, "The electronic properties of graphene," Rev. Mod. Phys. **81**(1), 109–162 (2009).
13. K. S. Novoselov, A. K. Geim, S. V. Morozov, D. Jiang, Y. Zhang, S. V. Dubonos, I. V. Grigorieva, and A. A. Firsov, "Electric field effect in atomically thin carbon films," Science **306**(5696), 666–669 (2004).
14. D. C. Elias, R. V. Gorbachev, A. S. Mayorov, S. V. Morozov, A. A. Zhukov, P. Blake, L. A. Ponomarenko, I. V. Grigorieva, K. S. Novoselov, F. Guinea, and A. K. Geim, "Dirac cones reshaped by interaction effects in suspended graphene," Nat. Phys. **7**(9), 701–704 (2011).
15. L. Wu, H. S. Chu, W. S. Koh, and E. P. Li, "Highly sensitive graphene biosensors based on surface plasmon resonance," Opt. Express **18**(14), 14395–14400 (2010).
16. S. W. Zeng, S. Y. Hu, J. Xia, T. Anderson, X. Q. Dinh, X. M. Meng, P. Coquet, and K. T. Yong, "Graphene-MoS2 hybrid nanostructures enhanced surface plasmon resonance biosensors," Sens. Actuators B Chem. **207**, 801–810 (2015).
17. L. M. Wu, Y. Jia, L. Y. Jiang, J. Guo, X. Y. Dai, Y. J. Xiang, and D. Y. Fan, "Sensitivity Improved SPR Biosensor Based on the MoS2/Graphene-Aluminum Hybrid Structure," J. Lightwave Technol. **35**(1), 82–87 (2017).
18. M. F. Ubeid and M. M. Shabat, "Numerical investigation of a D-shape optical fiber sensor containing graphene," Appl. Phys., A Mater. Sci. Process. **118**(3), 1113–1118 (2015).
19. C. Zhang, Z. Li, S. Z. Jiang, C. H. Li, S. C. Xu, J. Yu, Z. Li, M. H. Wang, A. H. Liu, and B. Y. Man, "U-bent fiber optic SPR sensor based on graphene/AgNPs," Sens. Actuators B Chem. **251**, 127–133 (2017).
20. X. C. Yang, Y. Lu, B. L. Liu, and J. Q. Yao, "Analysis of Graphene-Based Photonic Crystal Fiber Sensor Using Birefringence and Surface Plasmon Resonance," Plasmonics **12**(2), 489–496 (2017).
21. X. C. Yang, Y. Lu, L. C. Duan, B. L. Liu, and J. Q. Yao, "Temperature Sensor Based on Hollow Fiber Filled with Graphene-Ag Composite Nanowire and Liquid," Plasmonics **12**(6), 1805–1811 (2017).
22. A. N. Naimushin, S. D. Soelberg, D. U. Bartholomew, J. L. Elkind, and C. E. Furlong, "A portable surface plasmon resonance (SPR) sensor system with temperature regulation," Sens. Actuators B Chem. **96**(1-2), 253–260 (2003).

Biomedical Optics EXPRESS

23. Y. Tian, H.-y. Gao, Z. Wu, and M. Li, "Temperature characteristics of near infrared SPR sensors with Kretschmann configuration," Optoelectron. Lett. **11**(3), 191–194 (2015).
24. V. Bhatia and A. M. Vengsarkar, "Optical fiber long-period grating sensors," Opt. Lett. **21**(9), 692–694 (1996).
25. X. Huang, S. Li, J. S. Schultz, Q. Wang, and Q. Lin, "A MEMS affinity glucose sensor using a biocompatible glucose-responsive polymer," Sens. Actuators B Chem. **140**(2), 603–609 (2009).
26. D. C. Li, J. W. Wu, P. Wu, Y. Lin, Y. J. Sun, R. Zhu, J. Yang, and K. X. Xu, "Affinity based glucose measurement using fiber optic surface plasmon resonance sensor with surface modification by borate polymer," Sens. Actuators B Chem. **213**, 295–304 (2015).
27. B. Lu, X. Lai, P. Zhang, H. Wu, H. Yu, and D. Li, "Roughened cylindrical gold layer with curve graphene coating for enhanced sensitivity of fiber SPR sensor," in *Solid-State Sensors, Actuators and Microsystems (TRANSDUCERS), 2017 19th International Conference on* (IEEE, 2017), pp. 1991–1994.
28. C.-Y. Tan and Y.-X. Huang, "Dependence of refractive index on concentration and temperature in electrolyte solution, polar solution, nonpolar solution, and protein solution," J. Chem. Eng. Data **60**(10), 2827–2833 (2015).